Atom Indonesia

Journal homepage: http://atomindonesia.brin.go.id

Comparison of Electron Density and Absorption Dose Values of Artificial Boluses as Tissue Substitutes

D. R. Putri[1], F. K. Hentihu[2], R. J. Stevenly[3], E. R. Putri[1*]

[1]*Departement of Physics, Faculty of Mathematics and Natural Sciences, Mulawarman University, Barong Tongkok Streets, Samarinda, 75242, Indonesia*
[2]*Radiotherapy Installation, Lavalette Hospital, W.R. Supratman Streets, Malang, 65111, Indonesia*
[3]*Radiotherapy Installation, A. W. Sjahranie Hospital, Palang Merah Streets, Samarinda, 75128, Indonesia*

ARTICLE INFO

Article history:
Received 10 February 2025
Received in revised form 26 May 2025
Accepted 10 August 2025

Keywords:

Absorbed dose
Bolus
Electrons
Photons
Relative Electron Density (RED)

ABSTRACT

According to the Skin Cancer Foundation (SCF), approximately 1.8 million new cases of Squamous Cell Carcinoma (SCC) were reported globally in 2023. Radiotherapy remains a common treatment modality for SCC. However, delivering the maximum dose directly to the skin surface is often impeded by the skin-sparing effect of high-energy photon and electron beams. To overcome this limitation, a bolus, a tissue-equivalent material, is applied to bring the dose closer to the surface. This study aims to evaluate the electron density values derived from CT images and the absorbed doses of boluses fabricated from three different materials: resin Lycal 1079 (a propylene glycol-based compound), silicone rubber (polydimethylsiloxane), and plasticine (a mixture of stearate salt and glycerin). Dosimetric measurements were conducted using 6 MV photon beams and 12 MeV electron beams. Image analysis was performed using ImageJ and Matlab softwares. The irradiation setup employed a Source-to-Surface Distance (SSD) of 100 cm and a 10 × 10 cm² field size. Relative Electron Density (RED) values obtained from ImageJ for the resin and silicone rubber boluses were 1.007 and 1.188, respectively, while Matlab yielded RED values of 1.094 for resin and 1.194 for silicone rubber. For the plasticine bolus, both software tools produced a consistent RED value of 1.101. The findings indicate that beam energy has a significant impact on the absorbed dose at various phantom depths. Furthermore, all bolus materials increased the absorbed dose compared to setups without a bolus. Among the three materials, the resin bolus exhibited the most favorable characteristics, with a RED value closely approximating that of breast and skin tissue, highlighting its potential as an effective and economical tissue-equivalent bolus for clinical radiotherapy applications.

INTRODUCTION

Squamous Cell Carcinoma (SCC) is one of the most commonly diagnosed types of skin cancer worldwide [1]. SCC typically develops in areas of the body that are frequently exposed to Ultraviolet (UV) radiation from the sun, such as the head, neck, ears, lips, hands, and feet [2]. According to data from the Skin Cancer Foundation (SCF), approximately 1.8 million new cases of SCC are diagnosed globally each year [3]. One of the treatment options available in Indonesia for managing this type of cancer is radiation therapy or radiotherapy [4]. The principle of radiotherapy is to deliver the maximum radiation dose to the cancer or tumor while minimizing the dose to surrounding healthy tissues [5]. This goal is achieved using various techniques depending on the specific characteristics of the cancer, including its type, size, shape, and location [6]. However, when treating SCC with electron beam therapy, achieving the maximum dose at the skin surface can be challenging due to the skin-sparing effect [7]. The skin-sparing effect refers to the phenomenon where the radiation dose at the surface is lower and reaches its peak at a certain depth beneath the skin [8]. The problem can be resolved by employing

*Corresponding author.
E-mail address: erlinda.putri@fmipa.unmul.ac.id
DOI: https://doi.org/10.55981/aij.2026.1633

polymers. Since natural polymers tend to biodegrade, petrochemical-based synthetic polymers known as Bolus are preferred for this application [9]. To overcome this limitation and increase the surface dose, a tissue-equivalent material known as a bolus is commonly used [10]. A bolus is a material with properties similar to human tissue that is applied to the patient's skin during radiation therapy to modify the dose distribution [11]. It helps enhance the surface dose and ensures a more uniform distribution of radiation within the treatment area [12,13].

Previous research Nararta et al. (2022) compared the consistency of absorbed doses using boluses made from plasticine and silicone rubber [14]. The study utilized 10 MeV and 12 MeV electron beam energies. The results indicated that the deviation range in the absorbed dose consistency for plasticine was 0.002, whereas for silicone rubber it was 0.009. These findings suggest that the plasticine-based bolus offers better dose consistency over 25 fractionation sessions [14].

Cantika et al. (2022) conducted research by making silicon rubber and plasticine boluses with a size of 12 × 12 cm [15]. The energy used was 9 MeV and 12 MeV, and the thickness variation of each bolus was 0.5 cm, 1 cm, 1.5 cm, and 2 cm. The aim is to determine the best bolus material based on the parameters used, i.e., the absorbed dose value, electron density, and transmission factor. This study states that the silicon rubber bolus has a Relative Electron Density (RED) value that is close to the value of water density compared to the plasticine bolus. Silicon rubber and plasticine boluses can be said to be absorbent materials because the transmission factor values of the two boluses are below 100%. From the results of this study, the silicon rubber bolus is more capable of reducing the range of absorbed doses than the plasticine bolus. The density can be seen in Table 1 [16].

To calculate the electron density value, use the equation:

$$\rho^{w,e} = 1.0 + 0.001 \times N_{CT} \text{ for } -1000 \leq N_{CT} \leq 100 \quad (1)$$

$$\rho^{w,e} = 1.052 + 0.00048 \times N_{CT} \text{ for } N_{CT} > 100 \quad (2)$$

If the CT Number value owned by the bolus gets a value between -1000 and 100, Eq. (1) is used. However, if the CT Number value is more than 100, Eq. (2) is used [17].

Table 1. RED of human body organs against water [16].

Body Organs	RED (ρ)	Body Organs	RED (ρ)
Skin	1.078	Water	1.000
Breasts	1.014	Skeleton-cartilage	1.083

Another study was conducted by Rismawati et al. (2022), which aims to determine the impact of bolus thickness made from 3D printed Thermoplastic Polyurethane (TPU), silicon sealant, and resin using 10 MeV and 12 MeV energy [18]. They found that the three materials are similar to some soft tissues. Based on the material number value, the density of the material will be equivalent to a certain tissue. The TPU bolus with a thickness of 0.3 cm has a red color close to the value of water and then TPU with a thickness of 0.5 cm, resin with a thickness of 0.3 cm and 0.5 cm has a red color similar to the kidney and lung, while TPU and silicon sealant with a thickness of 1 cm have a red color similar to trabecular bone. Silicon sealants with a thickness of 0.3 cm and 0.5 cm have a red color that resembles the brain and breast. The silicon sealant has the highest flexibility of the two boluses as it has a milky white color and is easy to place on the uneven human body. In addition, the silicon sealant also produced the highest percentage increase in surface dose to the phantom.

Based on previous studies, the authors realize that there is something that can be studied, i.e., the utilization of 3D-printed bolus technology or patient-specific devices tailored to the anatomical shape of tumors or cancerous regions. This is good to do, but not all hospitals in Ind nesia can make boluses with a 3D printer. In this study, the authors want to make a bolus manually and economically with the basic materials of resin, silicon rubber, and plasticine to compare the comparison of electron density values and absorbed doses. This aims to compare the three bolus materials that have been made, which material is good as a substitute for skin tissue. The results of this study are expected to provide information about boluses that can be made manually for medical physicists in all hospitals in Indonesia.

In this study, a 6 MV photon beam was selected alongside a 12 MeV electron beam to evaluate the dosimetric performance of the fabricated boluses. The use of 6 MV photons is common in clinical practice due to their balanced characteristics, offering sufficient tissue penetration while maintaining an acceptable surface dose [19]. Unlike electron beams, 6 MV photons exhibit a skin-sparing effect, wherein the maximum dose (d_{max}) occurs several millimeters below the skin surface [20]. This makes them ideal for assessing the role of bolus materials, which are designed to overcome the skin-sparing limitation by shifting the dose buildup region closer to the surface [10]. The inclusion of 6 MV photon energy in this study allows for a clinically relevant comparison between photon and electron modalities, particularly in the treatment of superficial tumors, such as SCC in the head, neck, and skin regions [20]. Furthermore,

it demonstrates how manually fabricated boluses can optimize dose distribution in scenarios where 6 MV photon therapy is routinely used [21].

METHODS

In this study, in-house boluses were made from resin Lycal 1079 (a propylene glycol-based compound), night wax plasticine Shintoeng brand (a mixture of stearate salt and glycerin), with a size of 15 cm x 15 cm with a thickness of 1 cm, and a ready-made silicon rubber (polydimethylsiloxane) sheet bolus. The flowcharts of the manufacturing process of the boluses can be seen in Figs. 1(a) and (b).

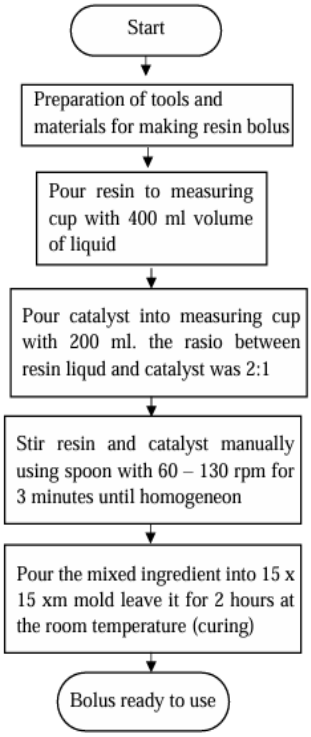

Fig. 1a. Flowchart of the manufacturing process resin bolus.

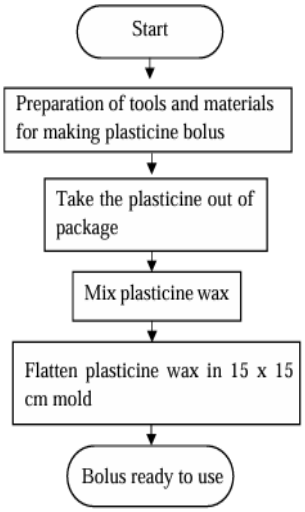

Fig. 1b. Flowchart of the manufacturing process of plasticine bolus.

Figure 2 illustrates the step-by-step procedure for fabricating the resin-based bolus. As shown in Fig. 2(a), 400 mL of resin liquid was measured using a graduated container. Subsequently, 200 mL of catalyst was measured separately, as indicated in Fig. 2(b), resulting in a resin-to-catalyst ratio of 2:1 by volume. The two components were then manually mixed using a spoon at an estimated speed of 60-120 rpm, as shown in Fig. 2(c), for approximately 3 minutes until a homogeneous mixture was achieved. The blended mixture was poured into a square mold measuring 15 × 15 cm (Fig. 2(d)) and allowed to cure at room temperature for 2 hours. Upon completion of the curing process, the hardened resin bolus was removed from the mold and deemed ready for clinical use (Fig. 2(e)).

Figure 3 depicts the fabrication process for the plasticine-based bolus. As shown in Fig. 3(a), two blocks of commercial night wax plasticine (Shintoeng brand) were prepared. The material was then removed from its packaging and pressed into a 15 × 15 cm mold, as illustrated in Fig. 3(b). In Fig. 3(c), the plasticine was kneaded thoroughly to ensure homogeneity and eliminate internal air voids, which could affect dose distribution. Finally, the bolus was shaped and smoothed to conform to the mold dimensions and was ready for application as shown in Fig. 3(d).

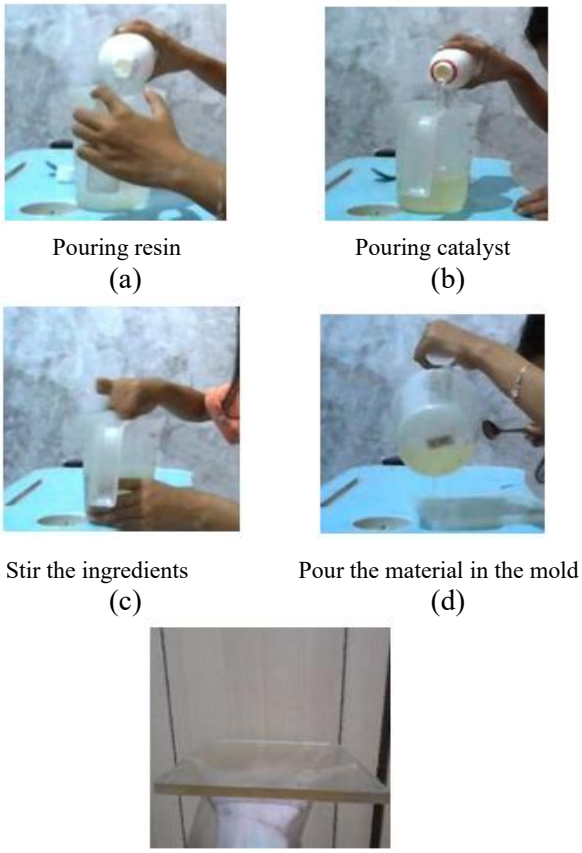

Fig. 2. Resin bolus manufacturing process.

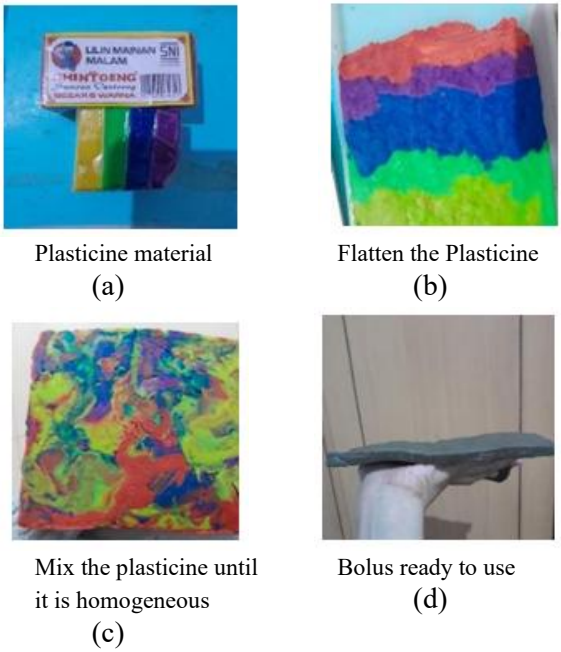

Fig. 3. Plasticine bolus manufacturing process.

Once the bolus was prepared, it was utilized to measure the absorbed dose and electron density. The absorbed dose was measured using a Farmer-type ionization chamber, which had been previously calibrated by the National Research and Innovation Agency (BRIN) at the Laboratory for Safety Technology and Radiation Metrology (LTKMR), Pasar Jumat, Lebak Bulus, South Jakarta, Indonesia. Figure 4 illustrates the equipment setup used during the data collection process, which included slab phantoms, an electrometer, a digital hygrometer-thermometer, a barometer, and a linear accelerator (linac). The electron density measurements were obtained from CT images [22].

The absorbed dose refers to the amount of energy deposited per unit mass in a medium by ionizing radiation [21]. The international unit for absorbed dose is the Gray (Gy), where 1 Gy is equivalent to 1 Joule/kg [23]. The absorbed dose values in this study were calculated using the Technical Report Series (TRS) 398 protocol, which is a standardized protocol developed for high-energy electron and photon beams. The equation used to determine the absorbed dose is as follows [20].

$$D_{D,W} = M_Q \times N_{D,W,Q} \times K_{Q,Q_0} \quad (3)$$

with $D_{D,W}$ is the absorbed dose in water at a given depth (cGy), M_Q is the dosimeter system reading at a given depth (nC), $N_{D,W,Q}$ is the water absorbed dose calibration factor (mGy/nC), and K_{Q,Q_0} is the detector correction factor between reference beam quality (Q_0) and actual measurement (Q) [20]. An illustration of the absorbed dose measurement set-up using a bolus is shown in Fig. 4.

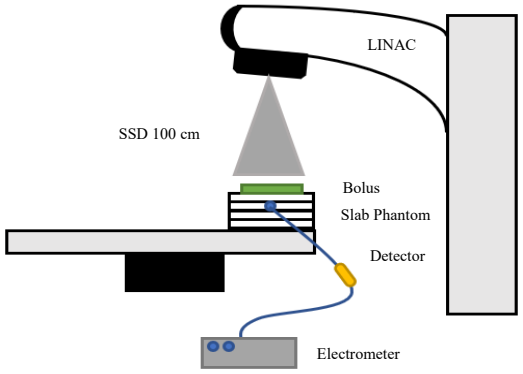

Fig. 4. Illustration of absorbed dose measurement set-up using a bolus.

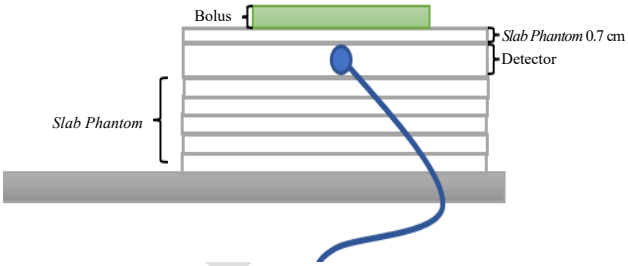

Fig. 5. Illustration of phantom depth.

Electron density measurements were conducted using a CT simulator located in the Treatment Planning System (TPS) room at the Radiotherapy Installation of A.W. Sjahranie Hospital, Samarinda. The CT number for each bolus was determined by calculating the average pixel value using ImageJ version 1.54 and Matlab R2021a. After obtaining the CT number, the RED values were calculated using Eqs. (1) and (2) to evaluate the tissue-equivalence of each bolus material. Repetition was done 3 times, and the average value was obtained.

The measurements were performed at various depths from the phantom surface, specifically at 0.7 cm, 1 cm, 1.5 cm, 2 cm, and 2.5 cm. These depths were chosen based on clinically relevant targets for radiotherapy treatment of tumors, such as SCC in regions including the head and neck, skin, and tongue. Since megavoltage (MV) photon beams from a linac are used, the maximum dose is not delivered at the surface, but within the build-up region, where the dose increases until it reaches the depth of maximum dose (d_{max}) [24].

Therefore, selecting depths from 0.7 cm to 2.5 cm enables evaluation of the absorbed dose received by tumors located in this build-up region [25]. This depth range reflects common clinical practice in superficial radiotherapy treatments and serves as a relevant reference for evaluating dose distributions for SCC and similar conditions [26]. An illustration of phantom depth variation is shown in Fig. 5. This range corresponds to the typical

build-up region where the d_{max} occurs in superficial radiotherapy treatment, providing a clinically relevant reference for SCC and similar conditions [27].

RESULTS AND DISCUSSION

The following are the results of CT Number and RED data using ImageJ and Matlab software, presented in the form of Table 2.

After determining the CT numbers of each bolus material, the RED values were calculated using two different software platforms. Before presenting the RED measurement results, it is important to highlight the basic chemical compositions of the bolus materials, as these directly influence electron density and absorption characteristics. Silicone rubber is a silicon-based polymer characterized by a backbone composed of alternating silicon (Si) and oxygen (O) atoms, with organic side groups such as methyl ($–CH_3$) or vinyl ($–CH=CH_2$) attached to the silicon atoms. In contrast, plasticine is typically formulated from a combination of bulking agents, petroleum jelly or white oil, starch, wax, stearic acid, sulfur, and zinc carboxylates. For the resin bolus, the RED values were found to be 1.076 and 1.085, respectively, both closely approximating the electron density of human skin, which is typically around 1.078. As presented in Table 2, this indicates the strong potential of the resin bolus to mimic skin tissue characteristics. In comparison, the silicon rubber bolus showed slightly higher RED values of 1.188 and 1.194, aligning more closely with the densities of spongy bone and femoral bone. These findings suggest that silicon rubber may be more representative of denser anatomical structures. The plasticine bolus yielded consistent RED values of 1.101 across both software tools, resembling the electron density commonly associated with cartilaginous tissues.

Given these results, the resin bolus emerges as the most tissue-equivalent among the three materials tested, particularly in relation to skin and breast tissue. This makes it a promising candidate for clinical applications where superficial tissue equivalency is critical. To further evaluate the dosimetric performance of each bolus material, absorbed dose calculations were performed using a 6 MV photon beam, with the results illustrated in Fig. 6.

Table 2. Results of CT Number and RED.

Bolus	ImageJ		Matlab	
	CT Number	RED (ρ)	CT Number	RED (ρ)
Resin	76.07	1.076	85.22	1.085
Silicon Rubber	284.59	1.188	292.10	1.192
Plasticine	102.57	1.101	102.95	1.101

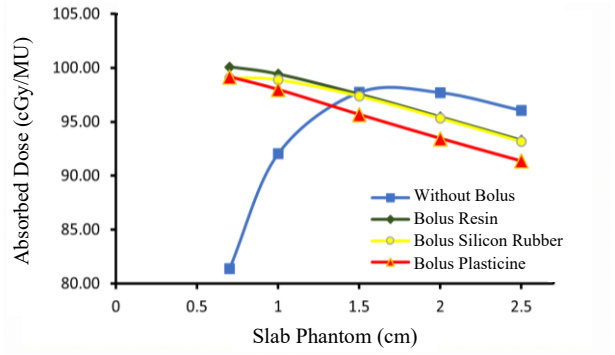

Fig. 6. Calculation of absorbed dose on bolus with 6 MV photon beam.

The absorbed dose data reveal clear differences in surface dose enhancement depending on the bolus material used. Without a bolus, the slab phantom alone yielded an absorbed dose of 81.39 cGy/MU at a depth of 0.7 cm. Introduction of the resin bolus significantly increased this value to 100.08 cGy/MU, representing a gain of 18.69 cGy/MU. Application of the plasticine bolus resulted in a dose of 99.17 cGy/MU, while the silicon rubber bolus achieved 99.06 cGy/MU. These findings highlight the bolus's ability to elevate surface dose, with the resin bolus demonstrating the highest enhancement.

These findings indicate that the use of a bolus during irradiation effectively increases the initial surface dose compared to using only the slab phantom. This confirms the bolus's function in mitigating the skin-sparing effect, wherein the surface dose is not at its maximum. The bolus enhances surface dose deposition, thus improving therapeutic outcomes in cases where superficial tumors are targeted.

At a depth of 1 cm, all bolus materials continued to enhance the absorbed dose relative to the slab phantom. However, by a depth of 1.5 cm, a slight reduction in dose was observed. While the slab phantom delivered 97.71 cGy/MU at this depth, the resin bolus resulted in 97.54 cGy/MU, with further reductions noted for silicon rubber (97.37 cGy/MU) and plasticine (95.67 cGy/MU). This trend persisted at greater depths, suggesting a shift in dose distribution away from deeper tissues.

This reduction in dose at greater depths suggests that bolus materials help confine the radiation dose to more superficial regions, preventing excessive dose delivery to deeper tissues. The use of a bolus, therefore, aligns with the core principle of radiotherapy: maximizing the dose to tumor tissue while minimizing exposure to surrounding healthy tissue. This is directly related to the concept of the skin-sparing effect. The observed dose reduction continues at depths of 2 cm and 2.5 cm, reinforcing the bolus's role in surface

dose optimization and deeper tissue protection. The following Fig. 7 illustrates the absorbed dose calculation graph for each bolus material when irradiated using a 12 MeV electron beam.

The subsequent analysis focuses on the comparison of absorbed dose calculations when boluses are applied under irradiation with a 12 MeV electron beam. Using only a slab phantom, the absorbed dose at a depth of 0.7 cm was measured at 97.65 cGy/MU. With the addition of a silicon rubber bolus, the absorbed dose increased significantly to 108.192 cGy/MU, reflecting a dose escalation of 10.542 cGy/MU. Following this, the application of a plasticine bolus resulted in an absorbed dose of 106.568 cGy/MU, while the use of a resin bolus yielded 105.061 cGy/MU.

The results clearly demonstrate that the application of a bolus consistently enhances the initial surface dose relative to setups without one. This enhancement is most evident at shallow depths, ranging from 0.7 cm to 1.5 cm, after which a gradual decline in absorbed dose is observed with increasing depth. The improved dose deposition in the superficial layers confirms the bolus' effectiveness in counteracting the skin-sparing effect, an inherent limitation of high-energy photon beams. By elevating the surface dose, the bolus ensures more effective coverage of superficial lesions, which is especially critical in breast, chest wall, or skin-involved tumor treatments. These findings align with clinical practice, where electron beams combined with bolus are most effective for treating superficial lesions within depths of approximately 1.5 cm, ensuring dose buildup at the surface while maintaining dose conformity. However, for cases requiring treatment depths around 2.5 cm, clinicians must carefully consider the rapid dose fall-off characteristic of electron beams to avoid underdosing the target volume while protecting underlying healthy tissues.

In contrast, dose distribution characteristics change significantly when using a 12 MeV electron beam. Due to the inherently high surface dose of electron beams, there is a minimal build-up region, and the maximum dose is typically reached near the surface. As shown in Fig. 7 (blue curve), when only a slab phantom was irradiated, the absorbed dose increased progressively, reaching 102.00 cGy/MU at a depth of 2 cm. However, the addition of bolus materials led to a slight dose reduction at the same depth. Specifically, the resin bolus produced an absorbed dose of 101.73 cGy/MU, followed by silicon rubber at 100.67 cGy/MU. The most notable reduction occurred with the plasticine bolus, which resulted in a dose of 85.54 cGy/MU. These variations reflect the bolus' influence on the electron beam's effective range and scattering behavior.

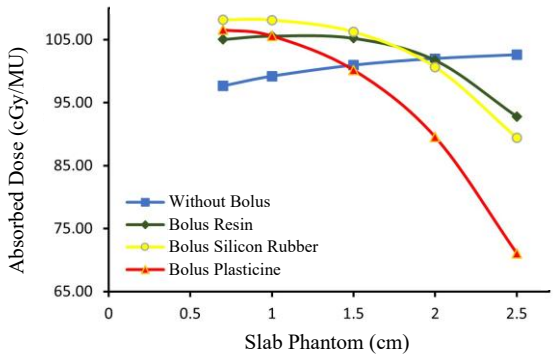

Fig. 7. Calculation of absorbed dose on bolus with 12 MeV electron beam.

These observations underscore the bolus's essential role in modulating dose distribution during radiotherapy. By enhancing surface dose while reducing unnecessary dose delivery to deeper tissues, bolus materials contribute to improved dose conformity and tissue sparing. This is particularly important in clinical scenarios where tumors are located near the skin surface and adjacent normal tissues must be protected. The ability of different bolus compositions to influence dose at various depths reinforces their value as practical tools for dose optimization and patient safety in both photon and electron beam therapy.

In light of these findings, further research should focus on refining manual fabrication methods to enhance the practicality and consistency of bolus application in clinical settings with limited resources. While this study demonstrates the dosimetric reliability of manually produced boluses, future work is needed to evaluate aspects such as long-term material durability, ease of shaping across various anatomical sites, and the potential for safe reuse after sterilization. Additionally, standardizing fabrication protocols could help ensure reproducible outcomes across different institutions. Exploring the adaptability of these bolus materials for use in pediatric cases, irregular anatomical contours, or in combination with immobilization systems may further broaden their clinical utility. These directions are particularly relevant for healthcare facilities where access to advanced manufacturing technologies is limited, supporting equitable radiotherapy practices globally.

CONCLUSION

This study has demonstrated that the application of bolus materials plays a critical role in enhancing surface dose during radiotherapy, effectively mitigating the skin-sparing effect associated with megavoltage photon and electron beams. Among the three materials evaluated, the

resin-based bolus consistently exhibited the most favorable characteristics for clinical use. Its RED values of 1.076 and 1.085 closely approximate those of skin and breast tissue, highlighting its potential as a tissue-equivalent substitute.

Furthermore, the resin bolus consistently yielded the highest increase in surface absorbed dose using both 6 MV photon and 12 MeV electron beams, without causing excessive dose escalation at greater depths. This characteristic ensures both effective tumor irradiation and protection of healthy tissues, aligning with the core principles of radiotherapy.

In conclusion, the manually fabricated resin bolus represents a practical, accessible, and cost-effective alternative to commercially available or 3D-printed bolus systems. Its clinical compatibility, dosimetric reliability, and material similarity to human soft tissue support its adoption in routine treatment workflows, particularly within resource-limited healthcare settings.

ACKNOWLEDGEMENT

We would like to express our sincere gratitude to the Radiotherapy Installation of A. W. Sjahranie Hospital, Samarinda, Indonesia, and the Radiotherapy Installation of Lavalette Hospital, Malang, Indonesia, for their generous support and provision of essential resources. Their contributions were instrumental to the successful completion of this research.

AUTHOR CONTRIBUTION

D. R. Putri and R. J. Stevenly contributed to data preparation and acquisition of data. D. R. Putri, E. R. Putri, and F. K. Hentihu were responsible for data analysis and interpretation. E. R. Putri and F. K. Hentihu conceived and designed the study.

REFERENCES

1. A. H. Roky, M. M. Islam, A. M. F. Ahasan *et al.*, Cancer Pathog. Ther. **3** (2025) 89.
2. L. Fania, D. Didona, F. R. Di Pietro *et al.*, Biomedicines **9** (2021) 171.
3. L. M. Wolden, Enhancing Skin Cancer Screening with Dermoscopy in Primary Care, Ph.D. Thesis, North Dakota State University (2023).
4. F. O. Stephens and K. R. Aigner, Basics of Oncology, Springer-Verlag, Berlin (2009) 1.
5. B. Ile, M. Spunei, I. Mălăescu *et al.*, *The Stability of Silicone Based Bolus Before and After A Radiotherapy Treatment*, in: AIP Conference Proceedings **2218** (2020) 030018-1.
6. N. Raghava, R. P. Raghava, L. Singh *et al.*, Plant Stress Toler. Physiol. Mol. Strateg. **16** (2016) 391.
7. J. Andersson, D. R. Bednarek, W. Bolch *et al.*, Med. Phys. **48** (2021) e671.
8. E. A. Kappos, A. Schulz, M. M. Regan *et al.*, BMJ Open **11** (2021) 1.
9. Barleany, H. Heriyanto, H. Alwan *et al*., Atom Indones. **48** (2022) 99.
10. F. M. Robertson, M. B. Couper, M. Kinniburgh *et al.*, J. Appl. Clin. Med. Phys. **22** (2021) 26.
11. V. Giacometti, R. B. King, C. McCreery *et al.*, Phys. Med. **92** (2021) 8.
12. J. A. Diaz-Merchan, S. A. Martinez-Ovalle, and H. R. Vega-Carrillo, Appl. Radiat. Isot. **199** (2023) 110899.
13. E. B. Podgorsak, *Treatment Machines for External Beam Radiotherapy,* in: Radiation Oncology Physics: A Handbook for Teachers and Students, IAEA, Vienna (2005).
14. M. D. Nararta, P. E. Juliantara, and C. Amelia, J. Soc. Res. **1** (2022) 558.
15. L. Chantika, V. F. Hanif, E. Defira *et al.*, J. Phys. Theor. Appl. **6** (2022) 25.
16. I. Yohannes, D. Kolditz, O. Langner *et al.*, Phys. Med. Biol. **57** (2012) 1173.
17. T. R. Möller, U. Rosenow, R. E. Bentley *et al.*, Use of Computers in External Beam Radiotherapy Procedures with High-Energy Photons and Electrons (ICRU Reports 42), ICRU, Bethesda (1987).
18. S. N. Rismawati, J. A. E. Noor, Y. Yueniwati *et al.*, Jurnal Penelitian Pendidikan IPA **8** (2022) 2833. (in Indonesian)
19. F. M. Khan and J. P. Gibbons, The Physics of Radiation Therapy, 5th ed., Lippincott Williams & Wilkins, Philadelphia (2014).
20. P. Andreo, M. S. Huq, M. Westermark *et al.*, Phys. Med. Biol. **47** (2002) 3033.
21. Ó. Gutiérrez, M. Prieto, A. Sanchez-Reyes *et al.*, Adv. Space Res. **69** (2022) 4376.
22. M. S. Al-Buriahi and B. T. Tonguc, Radiat. Phys. Chem. **166** (2020) 108507.

23. S. Wijokongko, Jeffri Ardiyanto, Fatimah *et al.,* Protokol Radiologi CT Scan dan MRI, Inti Medika Pustaka, Magelang (2019). (in Indonesian)

24. J. Zhang, G. Lu, and Z. You, Compos. Part B: Eng. **201** (2020) 108340.

25. A. Ashfaq, M. C. Clochard, X. Coqueret *et al.*, Polymers **12** (2020) 2877.

26. V. S. Averyn, *Short Refresher of Radiobiology*, in: Nuclear and Radiological Emergencies in Animal Production Systems, Springer, Berlin (2021) 13.

27. V. G. Tsirelson and R. P. Ozerov, Electron Density and Bonding in Crystals: Principles, Theory and X-ray Diffraction Experiments in Solid State Physics and Chemistry, CRC Press, Boca Raton (2020) 1.